A Sparse Nonlinear Model Predictive Control for Autonomous Space Missions

IAC-20,C1,3,3,x59155

A Sparse Nonlinear Model Predictive Control for Autonomous Space Missions

M. Pagone[a]*, M. Boggio[a], C. Novara[a], L. Massotti[b], S. Vidano[a]

[a] *Department of Electronics and Telecommunications, Politecnico di Torino, Corso Duca degli Abruzzi, 24, 10129, Torino, Italy*, michele.pagone@polito.it, mattia.boggio@polito.it, carlo.novara@polito.it, simone.vidano@polito.it
[b] *ESA/ESTEC, Keplerlaan 1, 2201 AZ Noordwijk, The Netherland*, luca,massotti@esa.int
* Corresponding Author

Abstract

Propellant consumption minimization is a key factor in space missions, as it strongly affects the duration of any mission. Nowadays, delta-V guidance strategies are obtained by means of classical ground based open loop methods, while academic research has mainly focused on autonomous low-thrust strategies. However, classical methods return instantaneous impulsive thrust actions that are not always feasible in practice, due to the technical limitations of real propulsion systems. In this paper, a novel Nonlinear Model Predictive Control framework for autonomous guidance and control with high-thrust quasi-impulsive maneuvers is presented. The internal prediction model is based on the so-called Modified Equinoctial Orbital Elements, which allow us to overcome relevant singularities given by the standard Keplerian elements. Different NMPC cost functions are compared in order to have a sparse thrust profile, minimizing at the same time the propellant consumption and the tracking error with respect to the target orbit. In particular, it is shown how the non-quadratic norms could achieve better performances. Finally, an Earth Observation mission, employing different NMPC functionals, is used as a benchmark and the results are compared with the ones coming from the classical astrodynamics solutions.

Keywords: Spacecraft, Control, Guidance, MPC, Autonomy, Nonlinear.

Nomenclature

ΔV: Delta-V
μ: Earth's planetary constant
g_0: Earth's gravity acceleration at sea level
I_{sp}: Specific impulse
J: Generic cost function
L: True longitude
m: Mass
r: Orbit radius
p: Semilatus rectum
T: Thrust
T_p: Prediction horizon
T_s: Sampling time
u: Acceleration
v: Velocity

Acronyms/Abbreviations

ECI: Earth-Centered Inertial
ESA: European Space Agency
MEOE: Modified Equinoctial Orbital Element
MIMO: Multi-input Multi-Output
MPC: Model Predictive Control
NMPC: Nonlinear Model Predictive Control
S/C: Spacecraft
SMA: Semi-major Axis

1. Introduction

Autonomous guidance and control strategies are key elements in the space industry in the view of future space missions. Indeed, they can significantly improve the capabilities of space vehicles to autonomously plan and perform complex maneuvers, reducing the effort in designing the missions on the ground and allowing to extend the spacecraft lifetime by minimizing the propellant consumption. In this context, the MPC is a very flexible approach for future applications of space guidance and control systems, thanks to its ability to manage linear and nonlinear systems, input and state constraints, MIMO systems and to optimize a wide class of performance indexes, allowing an efficient trade-off between performance and propellant consumption (see, e.g., [1, 2, 3]). The main idea behind the MPC-based guidance and control is to simplify the traditional mission planning carried out on ground, by means of the classical astrodynamics open-loop methods (e.g., using the Lambert's problem solution), designing a spacecraft capable to autonomously plan the required maneuvers and merging the guidance and control tasks.

In this context, the search for an optimum, in terms of guidance strategy and closed-loop control action, fits with the reduction of propellant consumption: each additional 'Newton' of thrust is paid with a substantial amount of propellant. Therefore, a significant research effort is focused on finding new classes of cost functions promoting the maximization of the satellite final mass. Differently from the numerous classical control problems for which the MPC was conceived, in space applications the propellant consumption usually represents the most important metric. From this point of view, the classic quadratic cost used in the MPC optimization problem

does not minimize the propellant consumption, as clearly shown by [4]. Furthermore, as discussed by [5], the drawbacks of the quadratic approach are that it leads to a sub-optimal propellant consumption and an undesirable continuous thrusting action.

When the plant and the constraints are linear, the MPC optimization can be tackled by means of convex programming (see, e.g., [6, 7]). In particular, [8] provide the explicit solution of model predictive control based on linear programming. These works inspired further developments, such as sparse MPC. Both [9, 10] propose a sparse linear MPC based on 1-norm cost function minimization., while [11] present a controller for a piece-wise affine system with 1-norm and ∞-norm minimization. A comparison between different cost indexes is carried out by [12, 13]. In the context of space maneuvering applications, [5] compares the classical quadratic cost function with a sum-of-norms. Other classes of performance indexes, based on LASSO regularization, are explored by [14, 15]. Nevertheless, the cited works are often limited to the case of linear (or linearized) dynamics and constraints. Furthermore, they have been mainly focused on autonomous low-thrust strategies.

In this paper, we propose a novel NMPC framework for guidance and control in space missions involving high-thrust quasi-impulsive maneuvers. A key feature of the proposed NMPC framework is that the internal prediction model is based on the so-called MEOEs. The advantage of using MEOEs are the following: (i) a generic reference trajectory can be generated just by assigning the orbital parameters, without specifying the satellite desired position along the orbit; (ii) the MEOEs are not significantly affected by singularity (the suffer of mathematical singularities only in the rare case of retrograde equatorial orbits); on the contrary, the classical Keplerian elements can be often undetermined, e.g., even when the orbit is equatorial and/or circular. The MEOE equations are intrinsically nonlinear and their linearization may lead to deteriorations of the control performance. This motivates the use of a nonlinear MPC approach, which is able to take advantage of the MEOE equations without requiring any linearization and/or approximation (provided that an effective nonlinear optimization solver is available). A second key feature of our NMPC approach is that it can use different kinds of cost functions, involving different signal norms, allowing us to obtain a sparse-in-time command input profile. This feature yields an improvement in terms of propellant consumption in high-thrust maneuvers with respect to the classical astrodynamics methods. Indeed, in these latter methods, the thrust profiles are based on an unfeasible abstraction: the concept of instantaneous and impulsive maneuver. Due to the technical limitation of the real propulsion systems, the ΔV budget cannot be concentrated in a single impulse: gravity and misalignment losses are introduced if no thrust vectoring and ΔV subdivision optimization are performed. On the contrary, our NMPC strategy is able to autonomously jointly optimize these two features.

As a case study, different NMPC configurations are employed for an Earth Observation mission, considering as baseline the ESA Sentinel-2 (within the Copernicus program) satellite. These kinds of missions expect one or more consecutive orbital plane changes, without any modification of SMA or eccentricity. They are suitable test benches for quasi-impulsive high-thrust guidance and control laws.

The paper is organized as follows. In Section 2, the classical NMPC theory is presented, and the modified cost functions are discussed. In Section 3, the S/C nonlinear dynamics is described by means of MEOEs. The simulations results are presented in Section 4, including also a trade-off between the different functionals introduced in Section 2. At last, the conclusions are drawn in Section 5.

2. Nonlinear Model Predictive Control

Consider the following nonlinear system:

$$\begin{aligned} \dot{x} &= f(x,u) \\ y &= h(x,u), \end{aligned} \tag{1}$$

where $x \in \mathbb{R}^{n_x}$, $u \in \mathbb{R}^{n_u}$, $y \in \mathbb{R}^{n_y}$ are the state, the input and the output respectively and the time dependence is kept implicitly. We assume that the state is measured, otherwise, an observer has to be employed, or a model in input-output form. The state is measured in real time, with a sampling time T_s. The measurements are $x(t_k),\ t_k = T_s k,\ k = 0, 1, \dots$. At time t, a prediction of the system state and output over the time interval $[t, t+T_p]$ is performed, where $T_p > T_s$ is prediction horizon. The prediction is obtained by integrating the equation (1). At time $\tau \in [t, t+T_p]$, the predicted output $\hat{y}(\tau) \equiv \hat{y}(\tau, x(t), u(t{:}\,\tau))$ is a function of the 'initial' state $x(t)$ and the input signal, whereas $u(t{:}\,\tau)$ denotes the input signal in the interval $[t, \tau]$. At each time $t = t_k$, we look for an input signal $u^*(t{:}\,\tau)$, such that the prediction $\hat{y}(\tau, x(t), u^*(t{:}\,\tau)) \equiv \hat{y}(u^*(t{:}\,\tau))$ has the desired behaviour for $\tau \in [t, t+T_p]$. Mathematically, at each $t = t_k$, the following optimization problem is solved:

$$\begin{aligned} & u^*(t{:}\,t+T_p) = \arg\min_{u(\cdot)} J\left(u(t{:}\,t+T_p)\right) \\ & \text{subject to:} \\ & \dot{\hat{x}}(\tau) = f(\hat{x}(\tau), u(\tau)), \quad \hat{x}(t) = x(t) \\ & \hat{y}(\tau) = h(\hat{x}(\tau), u(\tau)) \\ & \hat{x}(\tau) \in X_C,\ \hat{y}(\tau) \in Y_C,\ u(\tau) \in U_C. \end{aligned} \tag{2}$$

X_C, Y_C, and U_C are suitable sets describing possible constraints on the state, output, and input respectively. A receding control horizon strategy is employed: at a given time $t = t_k$, only the first optimal input is applied to the plant, the remainder of the solution is discarded. Then, the complete procedure is repeated at the next time $t = t_{k+1}$.

Remark. The optimization problem (2) is numerically non tractable, since $u(\cdot)$ is a continuous-time signal and thus, the number of decision variable is infinite. To overcome this issue, a finite parametrization of the input signal $u(\cdot)$ has been employed. In particular, we assumed a piece-wise constant parametrization, with changes of values at the nodes $\tau_1, \dots, \tau_{n_N} \in [t, t + T_p]$. Several simulations have been carried out considering the case study presented in Section 4, using values of n_N from 1 to 6. It has been observed that the value $n_N = 1$ leads to satisfactory behavior, without any significant performance degradation but with a reduced computational complexity with respect to the case $n_N > 1$. Hence, the value $n_N = 1$ (corresponding to a constant input for every $\tau \in [t, t + t_p]$) has been assumed for all simulation of Section 4.

2.1 Sparse Minimum Propellant Controller

Many works in the space control literature are nowadays focusing in refining the MPC theory for low-thrust applications. In this scenario, the S/C engines are expected to deliver a very low thrust magnitude for a huge amount of time. Conversely, few works deal with high-thrust mission profiles (e.g. the Hohmann's transfer), where the command action is delivered in a short time interval (quasi-impulsive maneuvers). The engines must be switched-on only in those points where changing the orbit shape requires a lower amount of propellant. An example: for raising the orbit apoapsis, the engines must fire tangentially to the orbit when the satellite is at the periapsis. The search for a sparse NMPC guidance and control strategy for impulsive maneuvers leads to consider and trade-off different cost functions. The most common MPC performance index is a weighted quadratic function of the predicted output tracking error $\tilde{y}_P$ and the system input u:

$$J_Q\left(u(t:t+T_p)\right) = \int_t^{t+T_p} \|\tilde{y}_P(\tau)\|_Q^2 + \|u(\tau)\|_R^2 \, \mathrm{d}\tau + \left\|\tilde{y}_P(t+T_p)\right\|_P^2. \quad (3)$$

The $\|x\|_W^2$ notation represents the (square) weighted norm of a vector $x \in \mathbb{R}^n$ such that $\|x\|_W^2 \doteq x^T \boldsymbol{W} x = \sum_{i=i}^n w_i x_i^2$ and $\boldsymbol{W} = \mathrm{diag}(w_1, \dots, w_n) \in \mathbb{R}^n$, $w_i \geq 0$. The predicted tracking error is $\tilde{y}_P(\tau) = r(\tau) - \hat{y}(\tau)$, whereas $r(\tau)$ is the desired reference to track and $\hat{y}(\tau)$ is obtained by integration of (1). The weights $\boldsymbol{Q} \geq 0, \boldsymbol{P} \geq 0$, and $\boldsymbol{R} > 0$ are diagonal matrix. Note that $\boldsymbol{Q}, \boldsymbol{P} \in \mathbb{R}^{n_y \times n_y}$ and $\boldsymbol{R} \in \mathbb{R}^{n_x \times n_x}$.

According to [8], the quadratic function (3) can be viewed as a sum of weighted mixed norms, one with respect to time and one with respect to space. We recall the definition of $\mathcal{L}_p$ signal norm in continuous time:

$$\mathcal{L}_p = \left(\int_a^b \|f(t)\|_q^p \mathrm{d}t \right)^{1/p} \quad (4)$$

Where $f: [a, b] \in \mathbb{R} \to \mathbb{R}^n$ is a measurable function and $1 \leq p \leq \infty$. Furthermore, $\|\cdot\|_q$ is the norm with respect to the space. Hence, the functional (3) can be viewed as a sum of $\mathcal{L}_2^2$ norms, plus a terminal constraint term, with $q = 2$.

Nevertheless, as shown by [4], the quadratic cost function does not exactly account for the propellant consumption, which, in space mission design, often represents the most important figure of merit. He demonstrates that the propellant penalty due to using the functional (3) goes from 18% up to 50%.

The variation of the satellite mass due to the firing of the engines is expressed by means of the Tsiolkovsky rocket equation:

$$\dot{m} = \frac{\|T\|_q}{I_{sp} g_0}. \quad (5)$$

Note that, $\|\cdot\|_q$ represents a suitable norm depending on engines mounting configuration (e.g. $q = 1$ for orthogonal thrusters, $q = 2$ for steering thrusters, and $q = \infty$ for a main engine with small steering thrusters, whose propellant consumption is negligible). Without loss of generality, the engine specific impulse can be considered constant throughout the whole thrusting interval. Then, the overall propellant consumption Δm is:

$$\Delta m = \frac{1}{I_{sp} g_0} \int_{t_0}^{t_f} \|T\|_q \mathrm{d}t. \quad (6)$$

From (6), a generic cost function, representing the propellant variation due to engines thrusting, can be written as:

$$J_m = \int_{t_0}^{t_f} \left(u_x(t)^q + u_y(t)^q + u_z(t)^q\right)^{1/q} \mathrm{d}t, \quad (7)$$

substituting the thrusting force T with the input acceleration u and expanding the q-norm. One can observe that the functional (7) is the $\mathcal{L}_p$ norm defined in (4), with $p = 1$ and $u(t)$ being a measurable function. Therefore, $J_m = \|u\|_{\mathcal{L}_p}$ and its minimization, according to Tsiolkovsky law, leads to the propellant mass

optimization. On the other hand, observing (3), if $q = 2$, $\boldsymbol{Q} = \boldsymbol{P} = \boldsymbol{0}$ and $\boldsymbol{R} = \boldsymbol{I}$ (i.e. the identity matrix), the cost function becomes:

$$J_Q = \int_{t_0}^{t_f} u_x(t)^2 + u_y(t)^2 + u_z(t)^2 \, \mathrm{d}t \, . \qquad (8)$$

Note that, J_Q corresponds to the square of $\mathcal{L}_2$ norm (i.e. $J_Q = \|u\|_{\mathcal{L}_2^2}$). Considering again $q = 2$, the (7) yields:

$$J_m = \int_{t_0}^{t_f} \left(u_x(t)^2 + u_y(t)^2 + u_z(t)^2\right)^{1/2} \, \mathrm{d}t. \quad (9)$$

It is clear how (8) does not represent the propellant consumption, being $J_Q \neq J_m$.

In this paper, we focus in studying a mixed $\mathcal{L}_1 \backslash \mathcal{L}_2^2$ functional:

$$J_Q\left(u(t: t+T_p)\right) = \int_t^{t+T_p} \|\tilde{y}_P(\tau)\|_Q^2 + \|\boldsymbol{R}u(\tau)\|_q \, \mathrm{d}\tau + \left\|\tilde{y}_P(t+T_p)\right\|_P^2. \qquad (10)$$

This formulation allows to optimize the propellant consumption and to design a sparse-in-time controller with a bang-bang structure. This is also due to the well-known property of 1 -norm minimization, which promotes sparsity in solution. The sparsity-in-time and the bang-bang behavior of the input signal are fundamental in view of the propellant consumption minimization for quasi-impulsive high-thrust space missions: (i) sparsity of the command allows the engine to avoid long periods of deadbeat low-thrust activity; (ii) bang-bang thrust profile allows the engine to exert the maximum thrust magnitude in those points along the orbit, where maneuvering is cheaper, cutting off the undesirable and expensive finite-time transient between the zero and the maximum thrust.

Definition. A controller is said 'bang-bang' when each component of its output can only assume a null, a maximum or a minimum value. The resulting command signal is piece-wise constant in time.

From (10), we are also interested in trading-off the different engine configurations. Indeed, the unique free variable is the q -norm relevant to the input activity function $b(u)$. With this approach, four different cases are studied and compared:

- The standard quadratic term. Q-NMPC: $b(u) = \|u(\tau)\|_R^2$, only for reference purpose.
- 1-NMPC: $b(u) = \|\boldsymbol{R}u(\tau)\|_1$.
- 2-NMPC: $b(u) = \|\boldsymbol{R}u(\tau)\|_2$.
- ∞-NMPC: $b(u) = \|\boldsymbol{R}u(\tau)\|_\infty$.

Each spatial norm $b(u)$ represents a different S/C engine mounting configuration (see, e.g. [4, 5]). The weights $\boldsymbol{R}$, $\boldsymbol{P}$, and $\boldsymbol{Q}$ are tuned in order to guarantee the maximum level of performance. Note that, in the case of no constraints on the state and/or on the output and if not interested in any transient behavior of the system, $\boldsymbol{Q}$ can be considered null. In summary, we are interested in avoiding long periods of parasite low-thrust and in promoting a sparse-in-time control action.

3. Spacecraft Dynamics

Consider a S/C of mass m_1 orbiting about a body of mass m_2, with $m_2 \gg m_1$. The S/C orbital dynamics is described by the two-body equation:

$$\dot{r} = -\frac{\mu r}{\|r\|_2^3} + \frac{T+F}{m_1} \qquad (11)$$

where r is the S/C position in ECI J2000 inertial reference frame, T is the thrust delivered by the engines, and F is the sum of all non-Keplerian perturbations. Note that, the S/C dynamics may be also uniquely determined by a set of six orbital parameters (also known as Keplerian orbital elements): semi-major axis, inclination, eccentricity, right ascension of ascending node, argument of periapsis and true anomaly. When the gravity is the only force acting on S/C, the first five orbital elements keep constant in time, whilst the true anomaly, describing the S/C position along the orbit, changes [16]. Nevertheless, this set suffers of singularities when the orbit is circular and/or equatorial. Thus, we introduce a set of six non-singular parameters: the modified equinoctial orbital elements (see, e.g. [17]). The relationship between the Keplerian parameters and the MEOEs is well described by [18].

In summary, the S/C dynamics consists in a nonlinear MIMO system with seven state variables: six describing the orbit shape and orientation and the last on describing the mass variation due to engines firing (see (5)). The state vector is $x = [p, f, g, h, k, L, m]^T$ (and the output y coincides with the state). Recalling (2), the following set is defined on the input:

$$U_c = \left\{u \in \mathbb{R}^3 : \|u\|_q \leq u_{max}\right\} \qquad (12)$$

where u_{max} is the maximum acceleration exerted by the selected thrust engines and $q = 1, 2, \infty$.

In formulae, the dynamics can be described as follows:

$$\begin{cases} \dot{p} = \dfrac{2p}{w}\sqrt{\dfrac{p}{\mu}}u_T \\ \dot{f} = \sqrt{\dfrac{p}{\mu}}\left[u_R \sin L + [(w+1)\cos L + f]\dfrac{u_T}{w} - (h\sin L - k\cos L)\dfrac{g u_N}{w}\right] \\ \dot{g} = \sqrt{\dfrac{p}{\mu}}\left[-u_R \cos L + [(w+1)\sin L + g]\dfrac{u_T}{w} + (h\sin L - k\cos L)\dfrac{g u_N}{w}\right] \\ \dot{h} = \sqrt{\dfrac{p}{\mu}}\dfrac{s^2\cos L}{2w}u_N \\ \dot{k} = \sqrt{\dfrac{p}{\mu}}\dfrac{s^2\sin L}{2w}u_N \\ \dot{L} = \sqrt{\mu p}\left(\dfrac{w}{p}\right)^2 + \dfrac{1}{w}\sqrt{\dfrac{p}{\mu}}(h\sin L - k\cos L)\,u_N \\ \dot{m} = \dfrac{\|T\|_q}{I_{sp}g_0}, \end{cases} \quad (13)$$

where $s^2 = 1 + h^2 + k^2$ and $w = 1 + f\cos L + g\sin L$ are auxiliary variables. Note that, the overall non inertial accelerations vector (i.e. non-Keplerian and thrusting accelerations) is given by $u = u_R\hat{\imath}_R + u_T\hat{\imath}_T + u_N\hat{\imath}_N$, where $\hat{\imath}_R$, $\hat{\imath}_T$, and $\hat{\imath}_N$ are unit vectors in radial, tangential, and normal direction according to the Frenet-Serret reference frame. The radial direction is considered positive pointing away from the Earth's centre, the tangential is measured positive in the direction of orbital motion and the normal direction is positive along the angular momentum vector of the satellite's orbit, according to a right-handed reference frame. Note also that, when the gravity is the only force acting on satellite, the first five differential equations of motion are $\dot{p} = \dot{f} = \dot{g} = \dot{h} = \dot{k} = 0$ and then, these MEOEs keep constant.

The satellite dynamics is perturbed by the Earth non-spherical gravitational acceleration, due to J_2 zonal gravity effect. In general, the J_2 perturbation has a slight effect on the eccentricity and the inclination. Whereas the major effects are focused on the right ascension of ascending node and the argument of the periapsis. Therefore, by accounting the map between the Keplerian orbital elements and the MEOEs (see [18]), the f, g, h, and k equinoctial parameters will result in a major perturbation due to Earth's oblateness.

4. Simulation Results

An Earth observation and monitoring mission can be viewed as one or more consecutive plane changes. The S/C, from a parking orbit, must overfly a precise coordinate on Earth ground, autonomously, for specific revisit needs or persistent monitoring (e.g. in case of disasters), and then return on the initial orbit (see, e.g., Fig. 1). In this work, only one plane change is accounted, i.e., a single monitoring maneuver is simulated. Note that, the plane changes consist in a simultaneous variation of inclination, right ascension of ascending node and argument of periapsis.

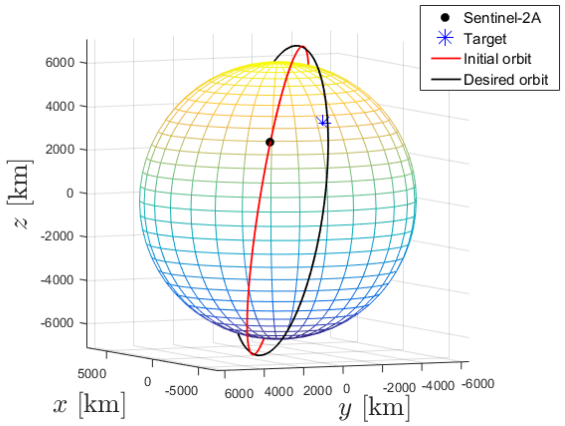

Fig. 1. Example of the mission scenario.

The ESA Sentinel-2 mission is the baseline for the case study. The satellite travels on a sun-synchronous orbit which ensures that it overflies any given point of the planet's surface at the same local mean Solar time. The orbit main features are reported in Table 1.

Table 1. Sentinel-2 orbit characteristics

	Value	Unit
Apogee	789.87	km
Perigee	788.06	km
Inclination	98.62	deg
Orbital Period	100.6	min
Revisit time	10	$days$

The satellite initial state $x_0 = [r_0, v_0, m_0]^T$ is:

- $x_0 = [-5.6331, 3.0100, 3.2298]^T \cdot 10^3 km.$
- $v_0 = [-2.3433, 2.6758, -6.5762]^T\ km/s.$
- $m_0 = 5000\ kg.$

and it represents the S/C parking orbit. When an alert is triggered on the on-board computer, the autonomous mission starts and the satellite moves on a different orbit, such that the point of interest on Earth's surface is overflown. Note that, the S/C initial mass has been increased with respect to the real Sentinel-2 case because,

if not considering a satellite constellation, a single S/C must be equipped with sufficient propellant provision for performing any commanded maneuver. In Table 2, the constant values used within the orbital simulator are highlighted.

Table 2. Simulation Constants

Description	**Symbol**	**Value**	**Unit**
Earth's Planetary Constant	μ	398600.4418	km^3s^{-2}
Earth's Gravity Acceleration	g_0	9.807	kms^{-2}
Earth's Mean Radius	R_E	6378.1	km
Engine Specific Impulse	I_{sp}	375	s

The goal is to design a maneuver which guarantees the satellite transfer, from the nominal orbit to the desired one, with the lowest propellant consumption and the highest precision. To this end, different types of cost functions are compared. The target orbit main parameters are presented in Table 3.

Table 3. Target orbit main parameters

Reference	Symbol	Value	Unit
Target	Long.	94.34	°
	Lat.	−38.49	°
Desired Orbit	p	7158.8	km
	f	5.7341×10^{-5}	−
	g	4.7424×10^{-4}	−
	h	1.1511	−
	k	−0.1657	−

The first step consists in tuning the NMPC parameters: the prediction horizon T_P and the $\boldsymbol{R}$, $\boldsymbol{P}$ and $\boldsymbol{Q}$ matrices. The tuning outcomes are shown in the Pareto diagram in Fig. 2. It consists in finding, among a series of feasible solutions of the same problem, the optimal one, such that it is impossible to make any improvement of the performance index without worsening another one. The following two merit indexed are considered:

- Normalized tracking error:

$$TE_n = \max_{j=1,\dots,T} \frac{\sum_{i=1}^{n} \left| R_{o_{ij}} - X_{ij} \right| / n}{\left\| R_{oj} \right\|_2}$$

- Normalized propellant consumption:

$$FC_n = \frac{m_0 - m_f}{m_0}$$

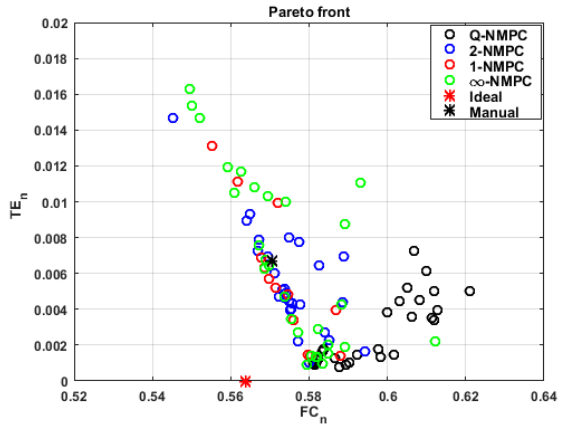

Fig. 2. Pareto Front.

where R_0 is the reference orbit, X is the post-maneuver orbit, $T = 2\pi\sqrt{a^3/\mu}$ the satellite orbital period, m_0 and m_f the S/C initial and final mass respectively.

The Pareto diagram is the outcome of the NMPC parameter tuning, with the four configurations of the input activity function $b(u)$, described in Section 2.1. Moreover, the results of the impulsive (but unfeasible) and of the quasi-impulsive realistic open-loop maneuvers are also reported for reference. Note that, the realistic open-loop maneuver has been carried out through the following approach:

- Computation of the required burning time Δt for a constant maximum thrust: $\Delta t = (m_0 v_e / T)(1 - \exp(-\Delta V / v_e))$.
- Application of the required ΔV in the interval $[t_0 - (\Delta t/2), t_0 + (\Delta t/2)]$, where t_0 is the time when the initial orbit intersects the target one. The S/C fires the maximum constant thrust in a direction that, instant by instant, is perpendicular to its tangential velocity.

The results are shown in Fig. 2. It is clear how all the NMPC configurations are able to provide better solutions with respect to the quasi-impulsive realistic maneuver, achieving not far performance indexes with respect to the ideal impulsive case. Furthermore, it is also possible to achieve a higher satellite final mass but increasing the tracking error.

Starting from the Pareto plot, one can pick the best solution for each NMPC configuration, whereby, it can be demonstrated how a sparse NMPC guarantees a wiser handing of ΔV subdivision during the maneuver. In Fig. 3 and Fig. 4 the thrust acceleration components, relevant to the best configuration (in terms of prediction horizon and weighting matrices) of Q-NMPC, 2-NMPC, 1-NMPC, and ∞-NMPC, are displayed. The cost functions without

the standard quadratic term results in a sparser control input and promoting a bang-bang thrust behavior.

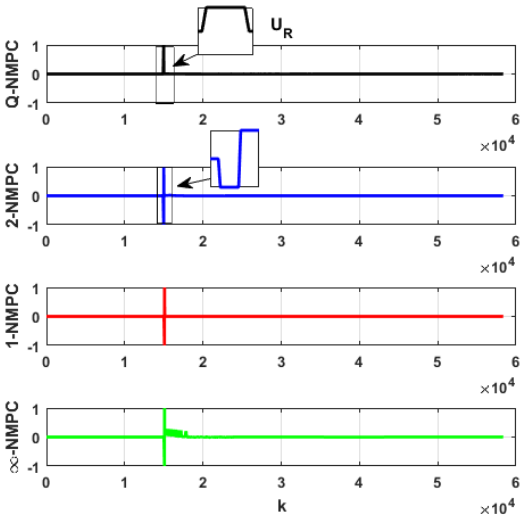

Fig. 3. Normalized radial thrust component.

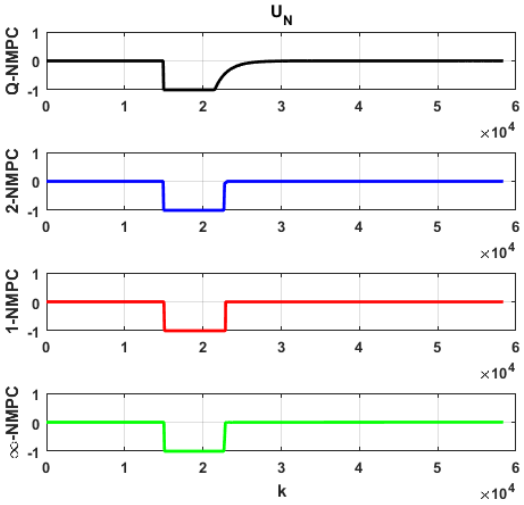

Fig. 4. Normalized normal thrust component.

The comparison of the propellant consumption is reported in Table 4.

Table 4. Propellant consumption comparison

Configuration	Propellant consumption [kg]	Ideal case deviation
Impulsive	2819	0%
Open-loop	2852.5	+1.19%
Q-NMPC	2906.2	+3.1%
2-NMPC	2819.5	+0.018%
1-NMPC	2838.2	+0.68%
∞-NMPC	2835.6	+0.59%

As expected, a sparse control input implies a better propellant efficiency. Indeed, the bang-bang control promotes the generation of an input signal which can switch only in three states: maximum, minimum and zero. Moreover, it is evident that the standard quadratic cost function leads to a worse propellant consumption with respect to both the sparse NMPC configurations and the quasi-impulsive open-loop case.

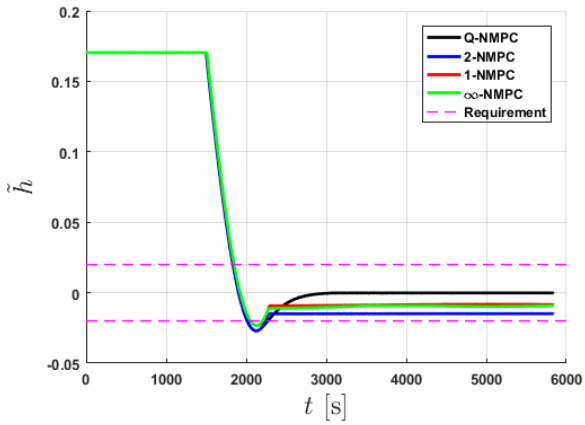

Fig. 5. Tracking error on h parameter.

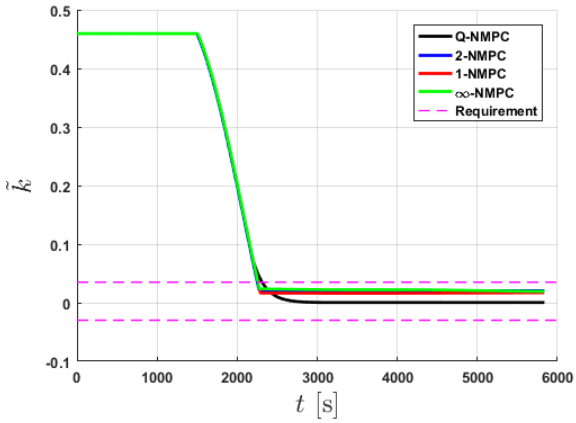

Fig. 6. Tracking error on k parameter.

In Fig. 5 and Fig. 6 the tracking error on the h and k equinoctial parameters are highlighted. They are the projection of ascending node vector onto the equinoctial reference frame and they are function both of the inclination and the right ascension of ascending node. These parameters are significantly worth of interest since, as aforementioned, the plane changes for the Earth observation and monitoring missions consist in a simultaneous variation of inclination, right ascension of ascending node and argument of perigee, whilst the shape of the ellipse does not change. For this reason, being the f and g elements the eccentricity vector projection onto the equinoctial reference frame, their possible tenuous

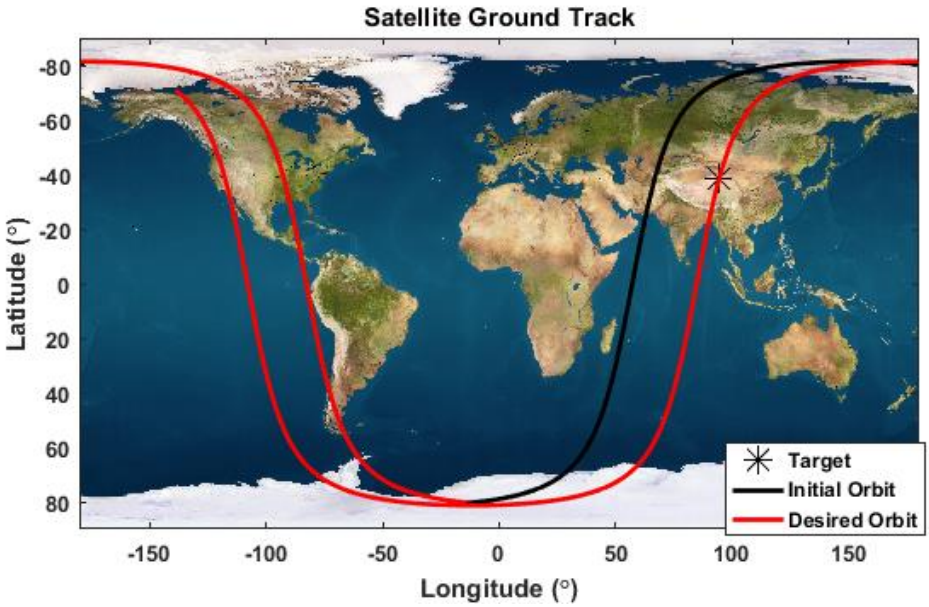

Fig. 7. Example of maneuver ground track.

variations do not affect the capability of the S/C to overfly and monitor the target.

An example of plane change maneuver ground track is shown in Fig. 7, while in Fig. 8 is reported the orbital plane change performed by the satellite. These latter figures prove that the S/C is able to overfly the alarm on Earth's surface with a sudden orbit plane change.

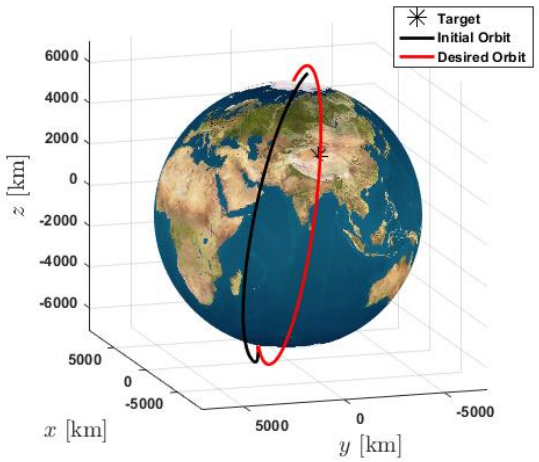

Fig. 8. Example of plane change maneuver.

6. Conclusions

The paper described how the concept of sparse-in-time control is suitable in designing the quasi-impulsive orbital maneuvers. In this regards, the standard NMPC cost function has been modified by substituting the quadratic term and, then, considering different vector norms of the command signal $u(t)$. Indeed, the standard approach results in a continuous command activity which leads to a sub-optimal propellant efficiency. Hence, an alternative approach has been proposed in order to produce the ΔV change in the shortest time. The resulting closed-loop behaviour shows both a bang-bang control profile and a sparse-in-time input signal, which are desirable properties for achieving the optimum propellant consumption. This approach has been implemented by comparing different NMPC configurations which are, afterwards, tested on an Earth observation and monitoring mission. The obtained results showed that the new proposed cost indexes achieve the proper features for designing a high-thrust space mission.

References

[1] E.N. Hartley, A Tutorial on Model Predictive Control for Spacecraft Rendezvous, European Control Conference, 15-17 July 2015.

[2] I. Breger, J.P. How, J_2-Modified GVE-Based MPC for Formation Flying Spacecraft, AIAA Guidance, Navigation and Control Conference, 15-18 August 2005.

[3] A. Weiss, I. Kolmanovsky, M. Baldwin, R.S. Erwin, Model Predictive Control of Three Dimensional Spacecraft Relative Motion, American Control Conference, 27-29 June 2012.

[3] I.M Ross, How to find minimum-fuel controllers, AIAA Guidance, Navigation and Control Conference and Exhibit, 15-19 August 2004.

[5] M. Leomanni, G. Bianchini, A. Garulli, A. Giannitrapani, R. Quartullo, Sum-of.norms model predictive control for spacecraft maneuvering, IEEE Control Systems Letters, Vol. 3, No. 3, July 2019.

[6] C.V. Rao J.B. Rawlings, Optimization strategies for linear model predictive control, IFAC Dynamics and Control of Process Systems, 1998.

[7] C.V. Rao J.B. Rawlings, Linear programming and model predictive control, Journal of Process Control, 10(2000), 283-289, 2000.

[8] A. Bemporad, F. Borelli, M. Morari, Model predictive control based on linear programming – the explicit solution, IEEE Transaction on Automatic Control, Vol. 47, No. 12, December 2002.

[9] S.K. Pakazad, H. Ohlsson, L. Ljung, Sparse control using sum-of-norms regularized model predictive control, 52nd IEEE Conference on Decision and Control, pp. 5758-5764, 2013.

[10] H. Ohlsson, L. Ljung, Trajectory generation using sum-of-norms regularization, 49th IEEE Conference on Decision and Control, December 15-17, 2010.

[11] J. Xu, T. van der Boom, L. Busoniu, B. De Schutter, Model predictive control for continuous piecewise affine systems using optimistic optimization, American Control Conference, July 6-8, 2016.

[12] M. Nagahara, D.E. Quevedo, Sparse representation for packetized predictive networked control, Proceedings of the 18th IFAC Word Congress, 2011.

[13] A. Dotlinger, R.M. Kennel, Near time-optimal model predictive control using an L1-norm based cost functional, IEEE Energy Conversion Congress and Exposition, September 14-18, 2014.

[14] M. Gallieri, J.M. Maciejowski, LASSO MPC: Smart regulation of over-actuated systems, Proceedings of the American Control Conference, June 2012.

[15] E.N. Hartley, M. Gallieri, J.M. Maciejowski, Terminal Spacecraft rendezvous and capture with LASSO model predictive control, International Journal of Control, 86:11, 2104-2113, 2011.

[16] E. Canuto, C. Novara, L. Massotti, D. Carlucci, C. Perez Montenegro, Spacecraft dynamics and control: the embedded control approach, Elsevier Aerospace Engineering Series, Oxford, England, UK, 2018.

[17] E.A. Roth, The Gaussian form of the variation-of-parameter equations formulated in equinoctial elements – Applications: Airdrag and radiation pressure, Acta Astronautica, Vol. 12, Issue 10, pp. 719-730, 1985.

[18] J.H. Jo, I.K. Park, N. Choe, M. Choi, The comparison of the classical Keplerian orbit elements, non-singular orbital elements (equinoctial elements), and the Cartesian state variable in Lagrange planetary equation with J_2 perturbation: part I, Journal of Astronomy and Space Science, 28(1):37-54, 2011.